Electronic Supplementary Information (ESI)

Z-scheme nanocomposite with high redox ability for efficient cleavage of lignin C−C bonds under simulated solar light

Xuejiao Wu,‡[a,b] Jinchi Lin,‡[a] Huizhen Zhang,[a] Shunji Xie,*[a] Qinghong Zhang,[a] Bert F. Sels*[b] and Ye Wang*[a]

[a]*State Key Laboratory of Physical Chemistry of Solid Surfaces, Collaborative Innovation Center of Chemistry for Energy Materials, National Engineering Laboratory for Green Chemical Productions of Alcohols, Ethers and Esters, College of Chemistry and Chemical Engineering, Xiamen University, Xiamen 361005, China. E-mail: shunji_xie@xmu.edu.cn; wangye@xmu.edu.cn.*

[b]*Centre for Sustainable Catalysis and Engineering, Faculty of Bioscience Engineering, KU Leuven, Heverlee 3001, Belgium. E-mail: bert.sels@kuleuven.be.*

‡These authors contributed equally to this work.

Detailed experimental procedures

Chemicals and Materials. All chemicals available commercially were purchased and used as received, unless otherwise noted.

Catalyst Preparation. Polymeric carbon nitride (PCN) was synthesized according to a thermal condensation method. Briefly, urea (10 g) was placed in a crucible with a cover and calcined in the muffle furnace at 550 ^{o}C for 3 hours (heating rate: 5 ^{o}C/min). Ag_3PO_4 powder was synthesized by the ion-exchange method. 2.3 mmol $AgNO_3$ was dissolved in 30 mL water, and 2.3 mmol Na_2HPO_4 in 5 mL water was then dropped into the solution under vigorous stirring. After stirring for 4 hours, the color of the product changed to yellow. The product was washed with distilled water three times and ethanol two times and dried at 70 ^{o}C in the air overnight.

Characterizations. Powder X-ray diffraction (XRD) patterns were recorded on a Panalytical X'pert Pro diffractometer using Cu K_α radiation (40 kV, 30 mA). SEM images were taken on a Hitachi S-4800 field emission scanning electron microscope. Diffuse reflectance Ultraviolet-visible (UV-vis) spectroscopic measurements were performed on a Varian-Cary 5000 spectrophotometer equipped with a diffuse reflectance accessory, the spectra were collected with $BaSO_4$ as a reference. X-ray photoelectron spectra (XPS) measurements were performed by a Quantum 2000 Scanning ESCA Microprobe (Physical Electronics) with Al-K_α radiation (1846.6 eV) and the spectra were referenced to the C 1s peak at 284.6 eV binding energy. The photoluminescence (PL) spectroscopic measurements were performed with a Hitachi F-7000 fluorescence spectrophotometer. Electron spin resonance (ESR) spectra were performed by a Bruker EMX-10/12 ESR spectrometer operated at X-band frequency at room temperature. The photoelectrochemical measurements were carried out with an electrochemical analyzer (CHI760E instruments, CHI, China) using a standard three-electrode system. The sample with a fixed amount of ~1 mg was coated onto an FTO glass electrode. The sample-coated FTO, Pt wire, and Ag/AgCl were used as the

working, counter, and reference electrodes, respectively. Na_2SO_4 aqueous solution (0.5 mol dm^{-3}) was used as the electrolyte.

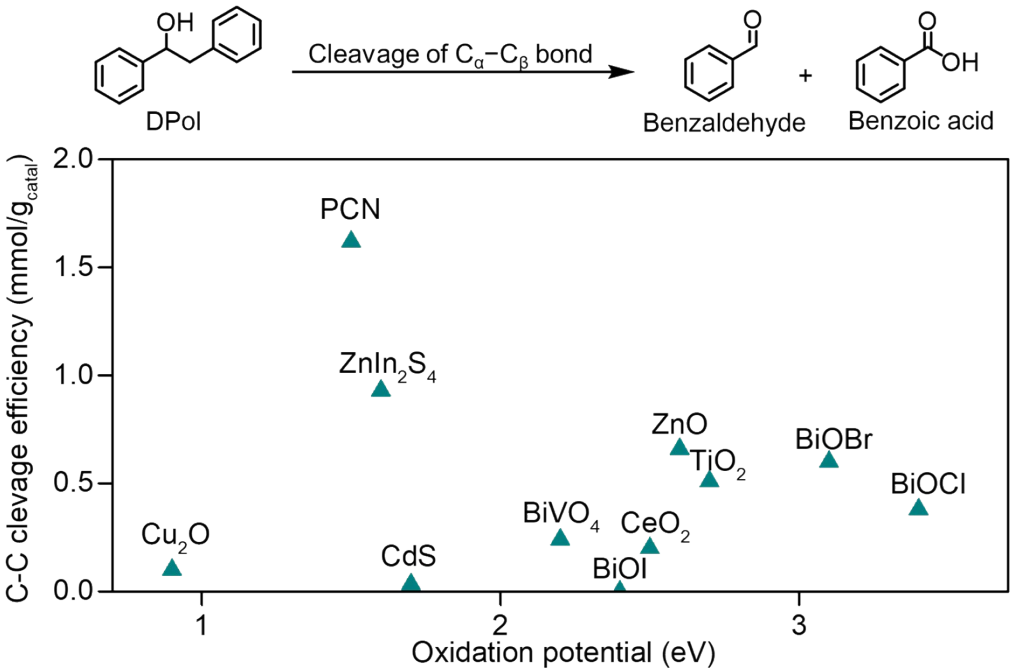

Fig. S1 Performances of typical semiconductors for photocatalytic cleavage of C_α–C_β bond in DPol and the corresponding valence band maximum values, i.e. oxidation potentials. C–C cleavage efficiency refers to the total yield of benzaldehyde and benzoic acid (in mmol) from the photocatalytic conversion of DPol over corresponding catalysts (per gram) after 6-hour reaction.

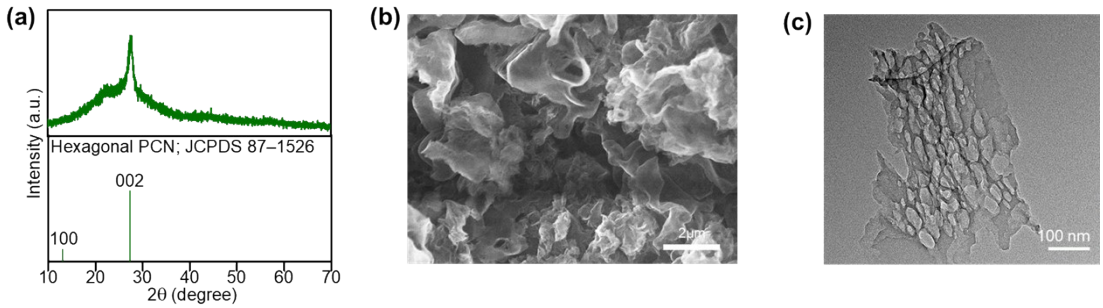

Fig. S2 Basic characterizations of PCN. (a) XRD patterns. (b) SEM image. (c) TEM image.

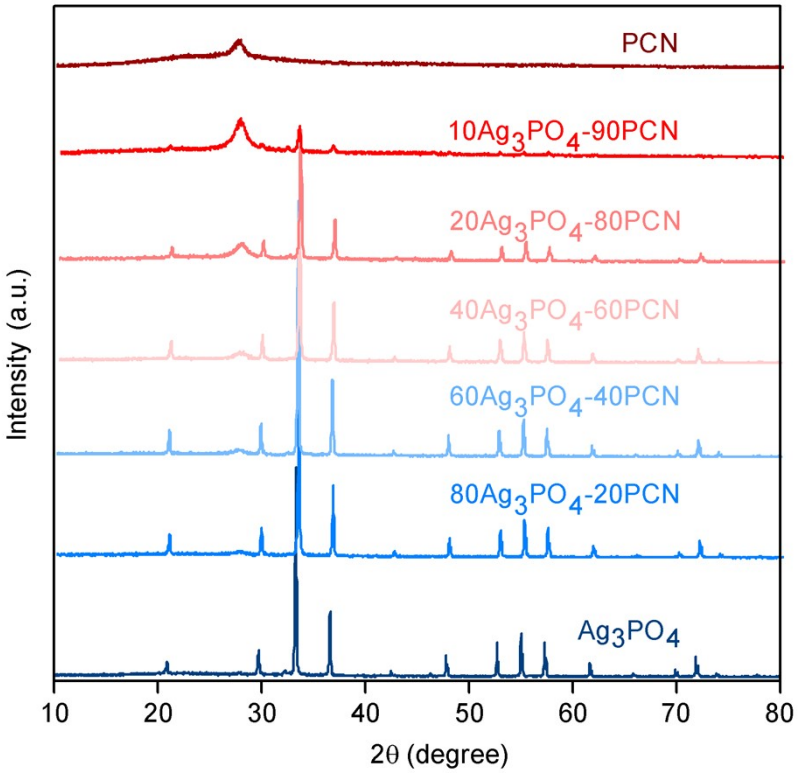

Fig. S3 XRD patterns of PCN, $10Ag_3PO_4$−90PCN, $20Ag_3PO_4$−80PCN, $40Ag_3PO_4$−60PCN, $60Ag_3PO_4$−40PCN, $80Ag_3PO_4$−20PCN, and Ag_3PO_4.

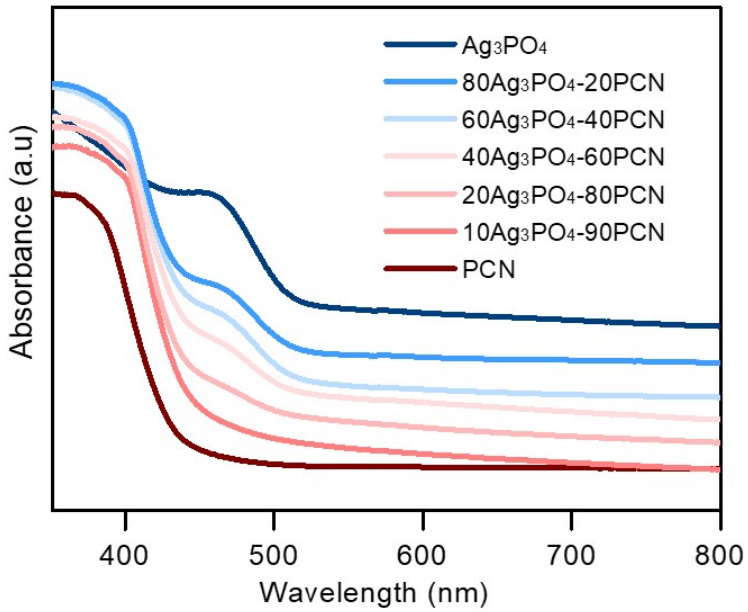

Fig. S4 UV-vis diffuse-reflectance spectra of PCN, $10Ag_3PO_4$−90PCN, $20Ag_3PO_4$−80PCN, $40Ag_3PO_4$−60PCN, $60Ag_3PO_4$−40PCN, $80Ag_3PO_4$−20PCN, and Ag_3PO_4.

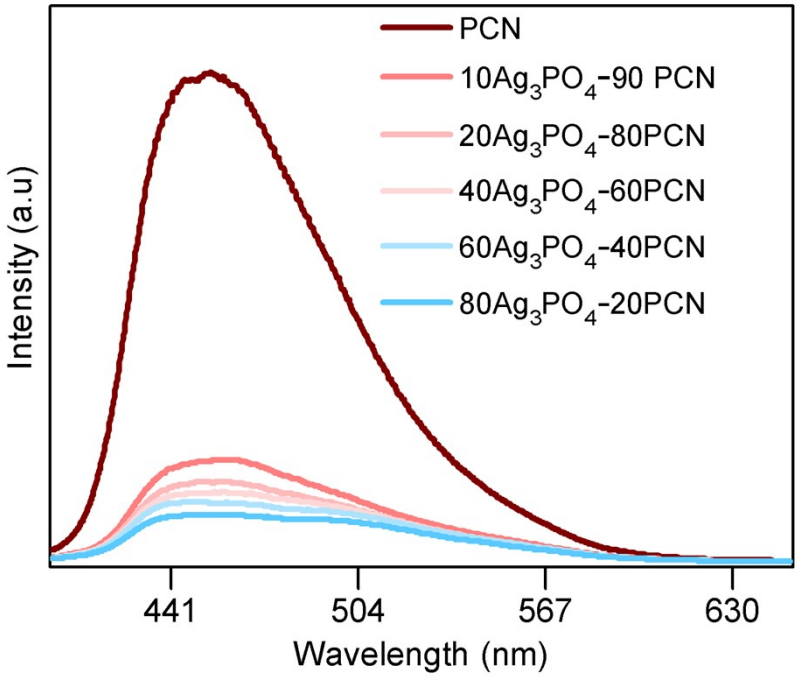

Fig. S5 Photoluminescence emission spectra of PCN, $10Ag_3PO_4$–90PCN, $20Ag_3PO_4$–80PCN, $40Ag_3PO_4$–60PCN, $60Ag_3PO_4$–40PCN, and $80Ag_3PO_4$–20PCN.

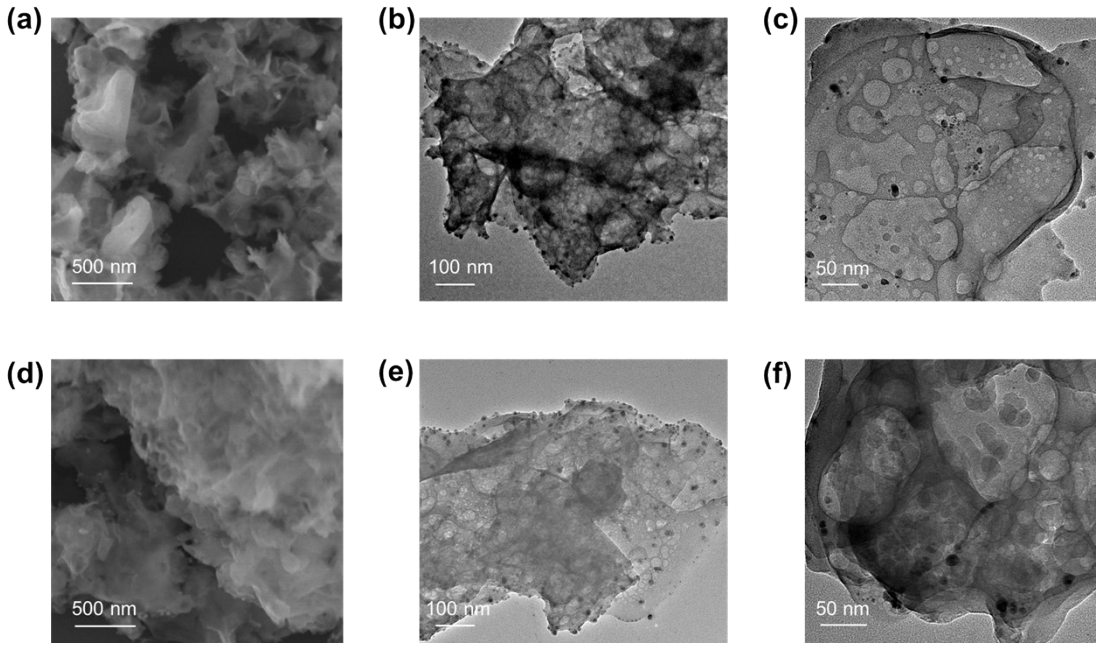

Fig. S6 (a) SEM and (b) (c) TEM images of $40Ag_3PO_4$−60PCN before reaction. (d) SEM and (e) (f) TEM images of $40Ag_3PO_4$−60PCN after reaction.

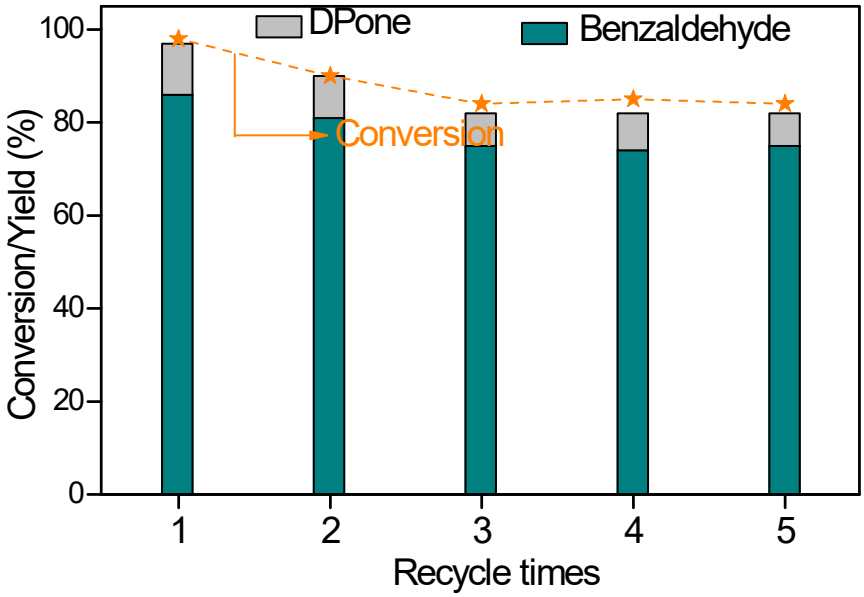

Fig. S7 Repeated uses of 40Ag_3PO_4−60PCN for the conversion of DPol.

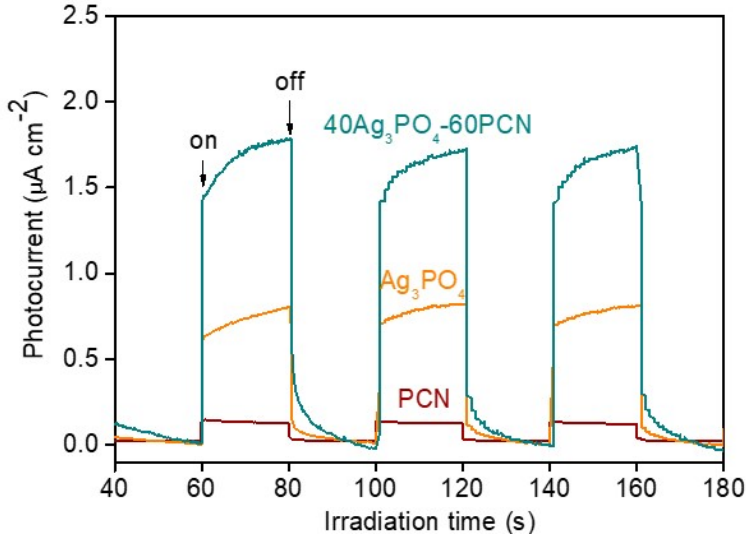

Fig. S8 Transient photocurrent responses of Ag_3PO_4, PCN, and $40Ag_3PO_4$−60PCN nanocomposite.

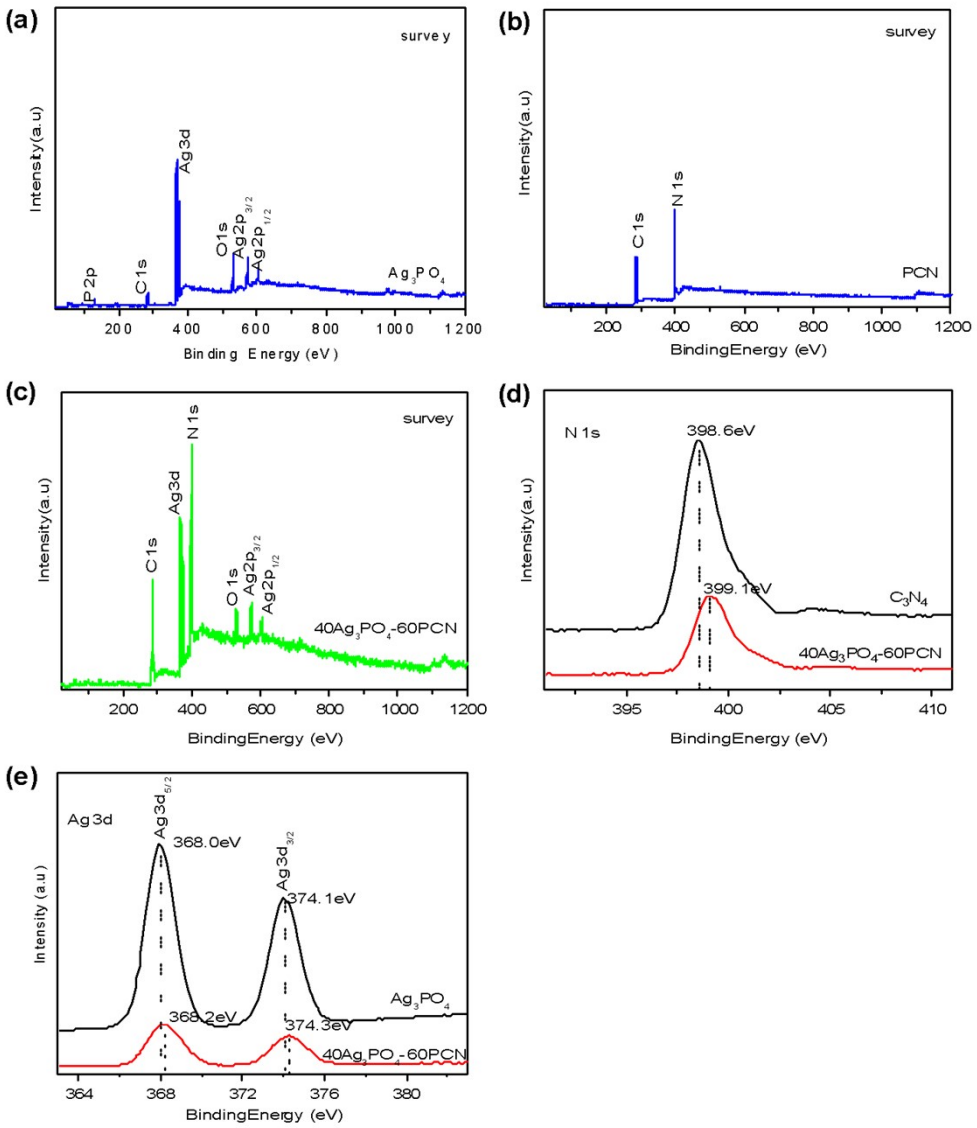

Fig. S9 XPS survey spectra of (a) Ag_3PO_4, (b) PCN, (c) $40Ag_3PO_4$−60PCN, and high-resolution XPS spectra of (d) N 1s of PCN and $40Ag_3PO_4$−60PCN nanocomposite, (e) Ag 3d of Ag_3PO_4 and $40Ag_3PO_4$−60PCN nanocomposite.

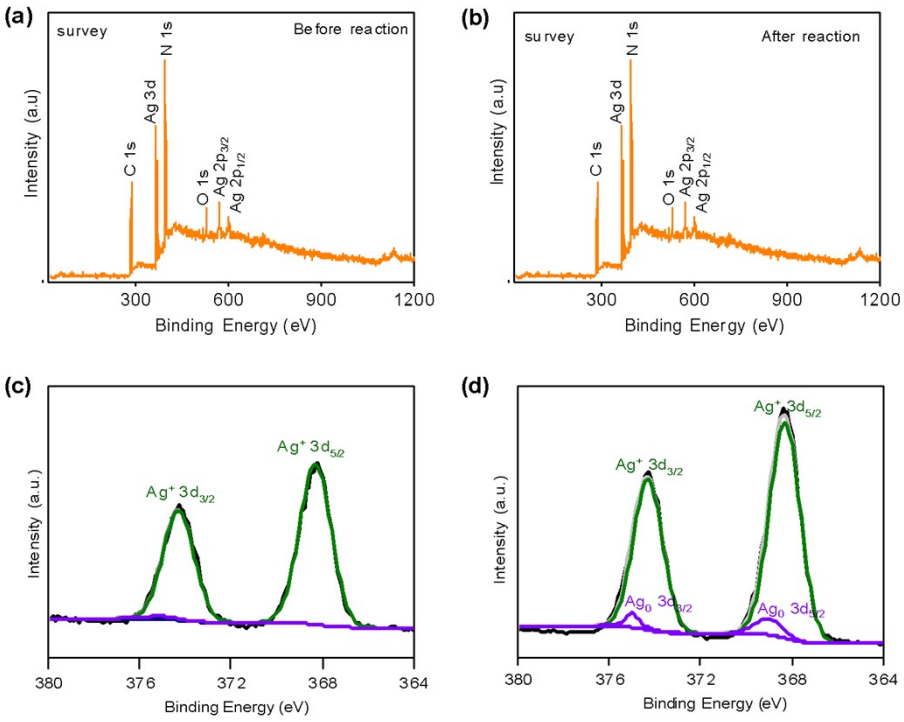

Fig. S10 XPS survey spectra of (a) $40Ag_3PO_4$−60PCN before reaction and (b) $40Ag_3PO_4$−60PCN after reaction, and Ag 3d core-level XPS spectra of (c) $40Ag_3PO_4$−60PCN before reaction and (d) $40Ag_3PO_4$−60PCN after reaction.

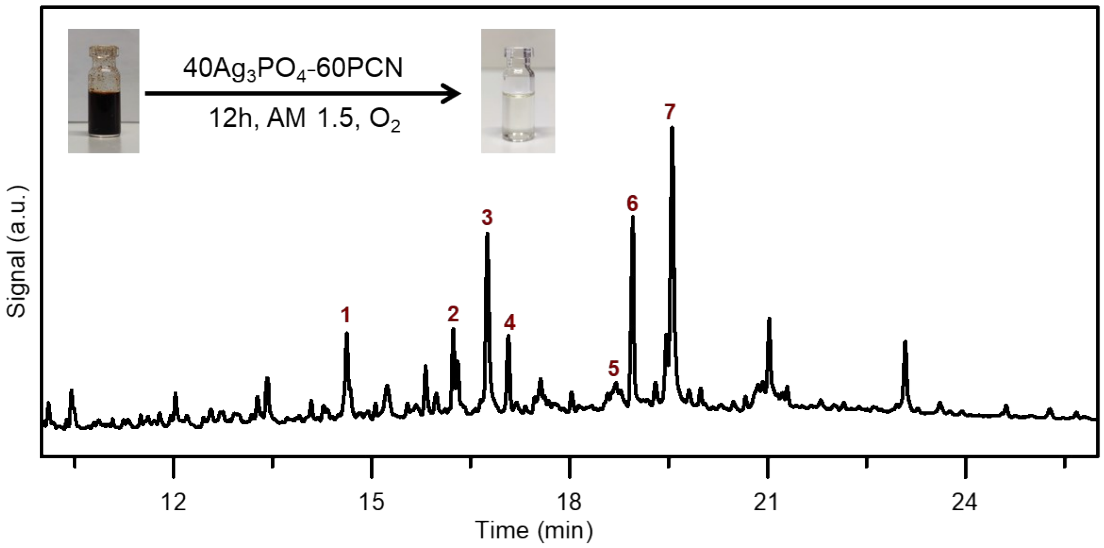

Fig. S11 GC spectrum of product mixtures obtained from the photocatalytic conversion of dioxasolv birch lignin. Insert images, solution of dioxasolv birch lignin before and after the reaction. The molecular structure of major products and corresponding mass spectra are listed in Fig. S12.

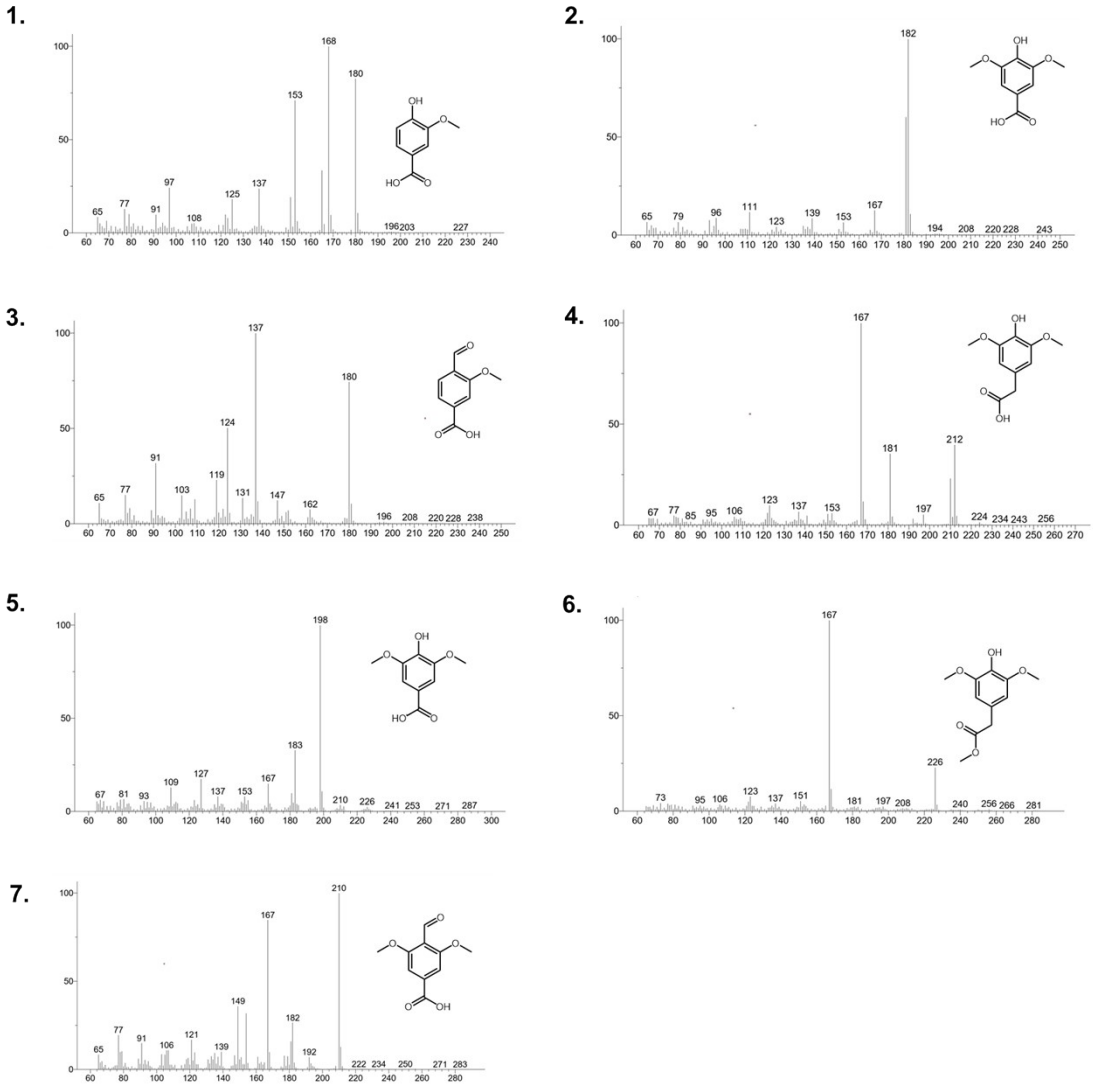

Fig. S12 Mass spectra of products from the photocatalytic conversion of dioxasolv birch lignin. These products are numbered by their sequence in GC list in Fig. S11.

Table S1. Band edge position of semiconductors used in this study.

Catalyst	VBM (V)	CBM (V)	Bandgap (eV)	Ref.*
TiO_2	2.7	-0.5	3.2	1
ZnO	2.6	-0.6	3.2	1
$ZnIn_2S_4$	1.6	-0.8	2.4	1
BiOBr	3.0	0.2	2.8	1
$BiVO_4$	2.2	-0.2	2.4	1
Cu_2O	0.9	-1.1	2	1
CeO_2	2.5	-0.4	2.9	2
BiOCl	3.4	0	3.4	3
BiOI	2.4	0.6	1.8	3
CdS	1.7	-0.7	2.4	1
PCN	1.5	-1.2	2.7	1

*References

1. W. Zhang, A. R. Mohamed and W.-J. Ong, *Angew. Chem. Int. Ed.*, 2020, **59**, 22894-22915.
2. T. B. Li, G. Chen, C. Zhou, Z. Y. Shen, R. C. Jin and J. X. Sun, *Dalton. Trans.*, 2011, **40**, 6751-6758.
3. R. Ma, S. Zhang, T. Wen, P. Gu, L. Li, G. Zhao, F. Niu, Q. Huang, Z. Tang and X. Wang, *Catal. Today*, 2019, **335**, 20-30.